Cataclasites in a fault zone exposed in a bedrock quarry near San Marcial, New Mexico, suggest multiple modes of deformation in interlayered sedimentary and volcanic rocks

Kevin M. Hobbs

2022, pp. 321-328. https://doi.org/10.56577/FFC-72.321

in:

Socorro Region III, Koning, Daniel J.; Hobbs, Kevin J.; Phillips, Fred M.; Nelson, W. John; Cather, Steven M.; Jakle, Anne C.; Van Der Werff, Brittney, New Mexico Geological Society 72nd Annual Fall Field Conference Guidebook, 426 p. https://doi.org/10.56577/FFC-72

This page is intentionally left blank to maintain order of facing pages.

New Mexico Geological Society Guidebook, 72nd Fall Field Conference, 2022, p. 321–328.

CATACLASITES IN A FAULT ZONE EXPOSED IN A BEDROCK QUARRY NEAR SAN MARCIAL, NEW MEXICO, SUGGEST MULTIPLE MODES OF DEFORMATION IN INTERLAYERED SEDIMENTARY AND VOLCANIC ROCKS

KEVIN M. HOBBS

New Mexico Bureau of Geology and Mineral Resources, 801 Leroy Place, Socorro, NM 87801; kevin.hobbs@nmt.edu

Abstract—In the southernmost outcrop of pre-Quaternary rock in the Chupadera Mountains, Socorro County, New Mexico, a down-to-the-south normal fault is exposed in a bedrock quarry just east of New Mexico State Road 1. Physical characteristics of this fault zone grant insight into timing and methods of faulting in a Rio Grande rift sub-basin that contains few fault outcrops. This quarry exposes silty sandstones of the Spears Group and the Andesite of Willow Springs, which are of similar upper Eocene age. The east wall of the quarry exposes the fault, where both the hanging and foot walls comprise andesite in a ~20 m wide fault zone around a 1.5 m wide fault core. Outcrop geometry suggests that the Spears Group sedimentary rocks are no more than ~10 m below the fault outcrop. Nearly all fractures in the fault zone are filled with cataclasized sedimentary rock showing physical and mineralogical similarities to the sedimentary rocks of the Spears Group. Cataclasites at the study site contain clasts with a smaller average diameter than the nearby Spears Group sediments, and microtextural observations suggest grain-to-grain comminution during faulting likely caused quartz spalling. Other features in the fault zone include zones of oxide clast concentration within cataclasites and post-faulting calcite vein mineralization.

INTRODUCTION

The geologic history of the San Marcial Basin, Socorro County, New Mexico, has been interpreted through its volcanic, sedimentary, and geomorphic records (e.g., Koning et al., 2020; Sion et al., 2020; Koning et al., 2021). Unlike adjacent Rio Grande rift basins to the north and south, the San Marcial Basin lacks a topographically well-expressed uplifted footwall block or basin-bounding horsts. Interpretations of its structural development therefore rely heavily upon gravity data (Gallant et al., this volume) or projection of faults from surrounding highlands (Cikoski et al., 2013). Little is known about the physical properties of these faults, largely because they are interpreted to exist under hundreds to thousands of meters' thickness of basin-filling siliciclastic sedimentary deposits. New observations presented here potentially can shed light on some aspects of San Marcial Basin tectonic development.

Central Rio Grande rift subsidence likely began in the middle Miocene (e.g., Chapin and Cather, 1994; Ricketts et al., 2016; Abbey and Niemi, 2020). Fault scarps in San Marcial Basin terrace sediments (Machette et al., 1998) indicate that local normal fault deformation continued at least until the middle Pleistocene. Total thickness of rift-filling sediments in the San Marcial Basin, and the inferred total displacement on basin-bounding fault systems, is unknown but likely at least hundreds of meters based upon thickness of basin-filling sedimentary deposits.

Faults and associated cataclasites in the southernmost Chupadera Mountains (Fig. 1) provide some insight into the brittle deformation processes that are partially responsible for San Marcial Basin subsidence. This paper presents data and interpretations from a fault zone encountered during geologic mapping of the Fort Craig 7.5-minute quadrangle in 2020. The primary focus of this paper is description of the features associated with the fault-related rocks at the study site. The characterization of deformation features that contribute to these faults' petrophysical properties and elucidate their tectonic history is a fundamental aspect of structural studies. Relations with and importance to larger-scale regional deformation deserve consideration due to limited fault outcrops in the San Marcial Basin.

GEOLOGIC SETTING

The study site is located 2 km south of the intersection of New Mexico State Road 178 and Interstate 25 in south-central Socorro County, New Mexico, in a disused (as of winter 2021) quarry at 33.72°N, 107.01°W (Fig. 1). The site is in the north-central San Marcial Basin and marks the southernmost exposure of bedrock associated with the Chupadera Mountains, a 30 km north-south oriented block of uplifted Proterozoic through Cenozoic rocks. Pertinent rocks exposed at the site include Upper Eocene fine sand–dominated sandstones of the Spears Group (hereafter "Tss," following the map unit nomenclature of Koning et al., 2021) and the Upper Eocene Andesite of Willow Springs (hereafter "Twa"). All of these units predate extensional deformation that led to the Rio Grande rift. They also predate all of the rift-filling siliciclastic sediments of the Santa Fe Group. Fault-related deformation features in the Santa Fe Group have been described by others (e.g., Rawling and Goodwin, 2003, 2006). In the eastern quarry wall, a normal fault striking approximately 150° and dipping 55°SW crosscuts Twa and incorporates Tss into the fault zone.

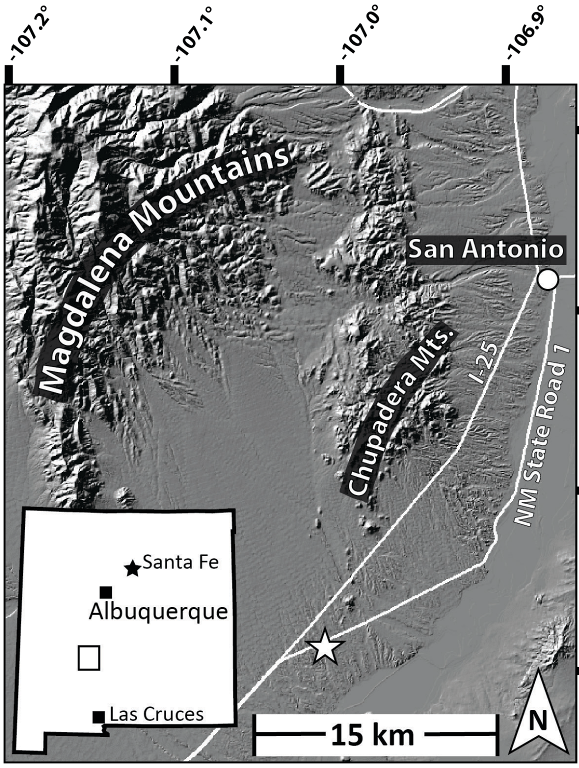

FIGURE 1. Hillshade digital elevation model map of study region shown in the inset box of the state of New Mexico. White star at bottom center marks study site and quarry location.

CATACLASIS AND BRECCIATION AT FAULTS

The characterization of distinctive rock types found in association with faults has led to increased understanding of the deformational environment, mechanisms of faulting, and associated faulting processes. These characterizations are well summarized by Sibson (1977), whose definition of cataclasis ("the brittle fragmentation of mineral grains with rotation of grain fragments accompanied by frictional grain boundary sliding and dilatancy") is used in this work. Cataclasis causes a reduction in average grain size in the materials accommodating strain (Engelder, 1974; Blenkinsop, 1991). In sandstones, as in most rocks, cataclasis is incremental, first causing few grain fractures while leaving most grains intact, and progressing toward highly deformed final stages where a small proportion of original grains are surrounded by a fine-grained matrix of crushed grain fragments (Engelder, 1974). The rate of cataclasite formation is dependent on material properties and strain rate; under high strain rate, single deformation events might cause complete fragmentation. The rock produced during cataclasis is termed cataclasite (Wise et al., 1984); its grain size is dependent on the grain size of the faulted material (i.e., cataclasite produced from shear in coarse-grained rocks might be coarser than that produced by faulting fine-grained rocks). Cataclasites form under cohesive but brittle rock conditions during faulting and are restricted to the upper 10–15 km of the crust (Sibson, 1977, 1986).

Fault breccias are assumed to have formed during shear or dilatancy in both cohesive and non-cohesive material at the time of faulting (Sibson, 1977). There have been many attempts at textural, genetic, and quantitative classifications of breccias (Laznicka, 1988; Jébrak, 1997; Woodcock et al., 2006; Mort and Woodcock, 2008). The semi-quantitative classification of Mort and Woodcock (2008) is applied in this study. Fault breccias have been assumed to have formed under lower confining pressure conditions and in less cohesive rocks than finer-grained cataclasites (Sibson, 1977, 1986), though multiple studies show both breccias and finer-grained cataclasites in the same fault zone (Hadizadeh et al., 1991; Davis et al., 2004; Luther et al., 2013; Bolognesi and Bistacchi, 2016). Given the non-uniform cohesive properties of interlayered rocks of differing lithologic composition such as the andesites and sandstones at the study site, and the likely spatial and temporal variations in pressure conditions at any fault, the presence of finer-grained cataclasites alongside fault breccias should not be surprising and is not necessarily indicative of different episodes of fault motion.

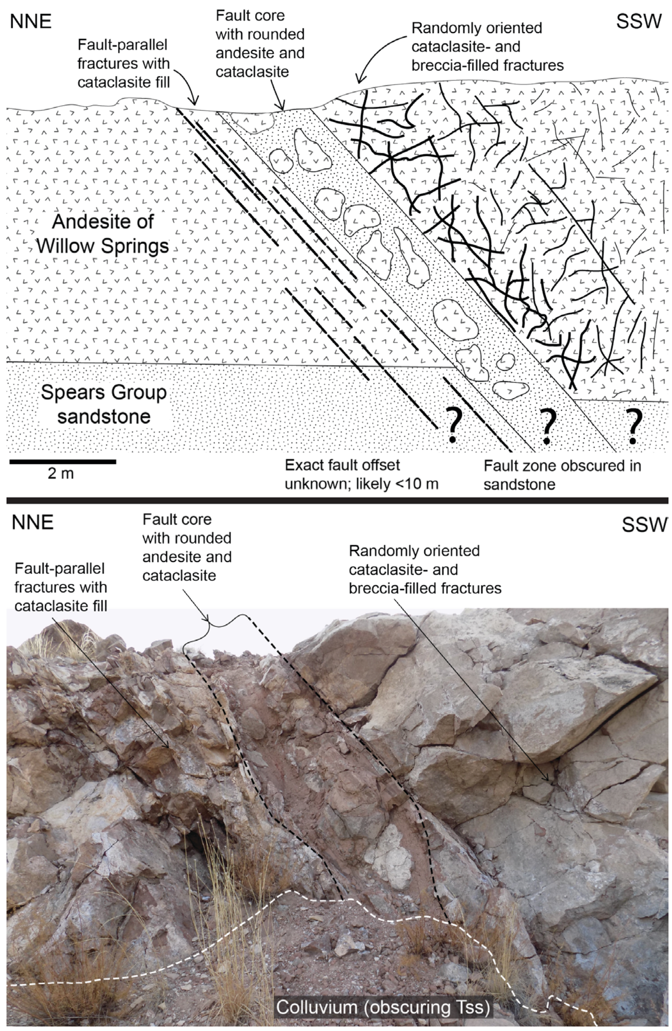

FIGURE 2. Top: Schematic cross section of geologic features at the eastern quarry wall at the study site. Spears Group sandstone is covered at the site; its depth is inferred from outcrops across the quarry to the west. Displacement along the fault is unknown. Bottom: Annotated photograph of fault zone at study site. Tss is not observed in outcrop in this quarry wall, but is exposed in the opposite quarry wall 35 m to the northwest. Scale for photograph is the same as that for the schematic above.

METHODS

Whole-rock samples were prepared for powder X-ray diffraction (XRD) analysis by crushing with mortar and pestle. XRD analyses were performed at the New Mexico Bureau of Geology and Mineral Resources on a Panalytical X'Pert Pro diffractometer emitting Cu K-alpha radiation at a 1.54 Å wavelength. Standard 30-micron thin sections were prepared by Wagner Petrographic. Standard transmitted light optical microscopy techniques were used. Presence of oxide minerals was verified with reflected light microscopy. The methods of Dickinson (1970) were applied to petrographic counts. Quantitative measurements of grain size on thin sections were performed with Olympus Stream software tools. Photomicrograph mosaics were created with Adobe Photoshop's Photomerge tool; colors were not altered.

RESULTS

Field Observations

The Andesite of Willow Springs (Twa) at the study site is a gray (average Munsell color 5YR 5/1) plagioclase-pyroxene phyric andesite porphyry with 15–30% phenocrysts of whitish plagioclase with 1–4 mm diameter and trace 5% phenocrysts of dark brownish-black pyroxene of 0.5–2 mm diameter. Sandstones of the Spears Group (Tss) at the study site are reddish-gray to reddish-brown (5YR 5/2, 5/3, 5/4, and 4/3) massive silty arenites. Koning et al. (2021) report an interbedded relationship between the Twa and Tss in the study area.

Deformation features associated with faulting at the study site extend laterally for approximately 20 m, with different expressions in the hanging wall, footwall, and fault core (Fig. 2). Throughout the outcrop, there are rare mm- to cm-scale calcite-filled fractures. These fractures crosscut all other structures and therefore are interpreted to postdate fault motion. Zoned growth patterns and µm-scale fluid inclusions (Fig. 3) are present in individual calcite crystals within the mineralized fractures.

The fault core is approximately 1.5 m wide and is well defined by sharp boundaries against the adjacent fault blocks. The fault core contains rounded boulders and cobbles of Twa; subangular to angular small cobbles through granules of Twa also are present. The majority of the volume of the fault core is occupied by material bearing textural (coarse silt through medium sand), color (Munsell colors 5YR 5/2, 5/3, 5/4, and 4/3; reddish gray and reddish brown), and compositional similarities to Tss, which is not exposed at the fault outcrop but exists no more than 10 m stratigraphically below Twa in the outcrop on the opposite quarry wall. Cobble- to boulder-sized blocks of sandstones of Tss are sometimes themselves brecciated in the fault core (Fig. 4). The fault core also contains rounded to subrounded clasts of andesite.

The footwall is marked by a 2–4 m wide zone of cataclasite-filled fractures that are parallel to the fault. Cataclasite in the footwall fractures is of the same composition, color, and texture as Tss. Twa between the fault-parallel, cataclasite-filled

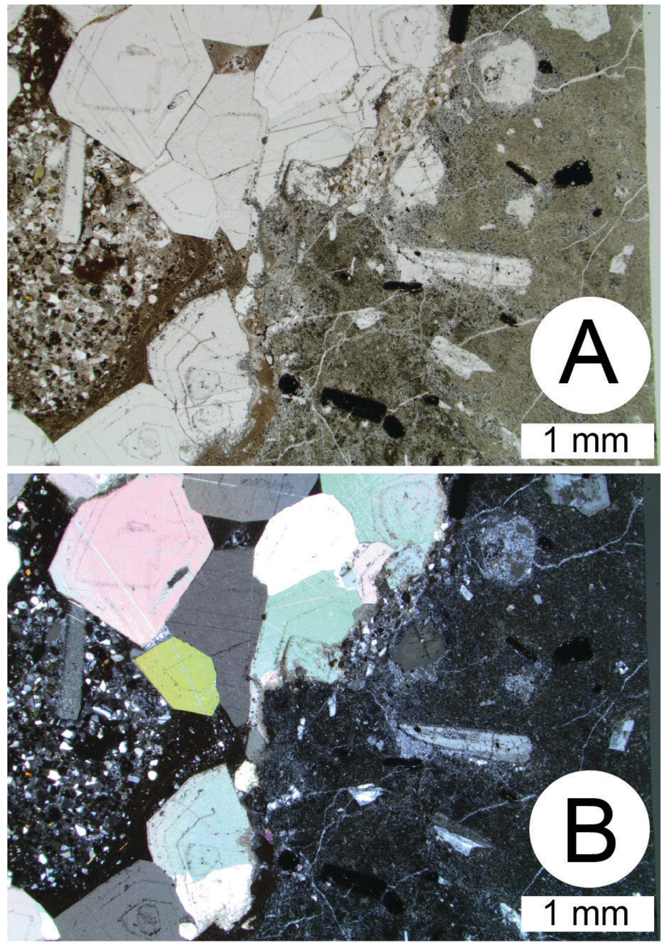

FIGURE 3. Plane light (A) and cross-polarized light (B) thin section photomicrographs of calcite-filled fractures in the fault zone. Fractured andesite with plagioclase phenocrysts occupies the righthand portion of the photomicrographs. Cataclasite comprising reworked individual clasts of Spears Group sandstones occupies the left center portion of the frame.

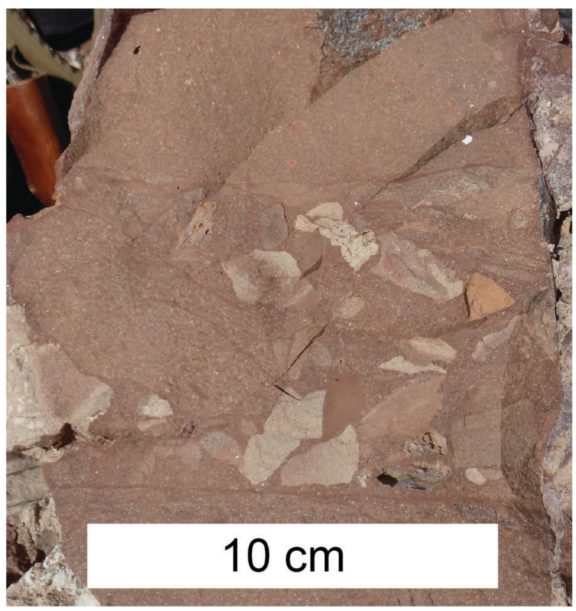

FIGURE 4. Brecciated Spears Group sandstone from within the fault core at the study site. Massive unbrecciated sandstone exists above and below the breccia zone.

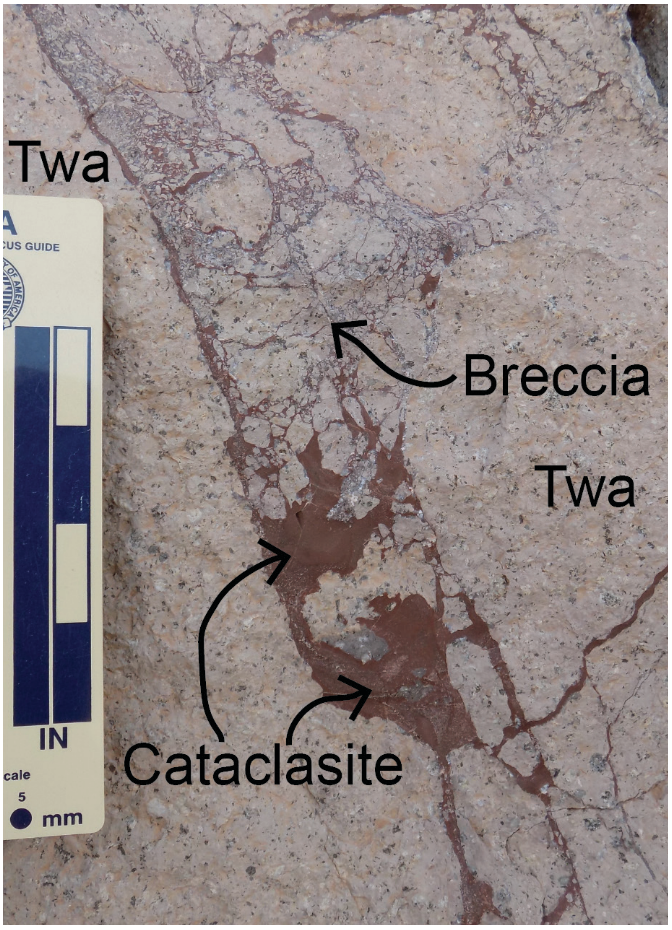

FIGURE 5. Cataclasite- and breccia-filled fractures in the fault zone hanging wall. Twa = Andesite of Willow Springs.

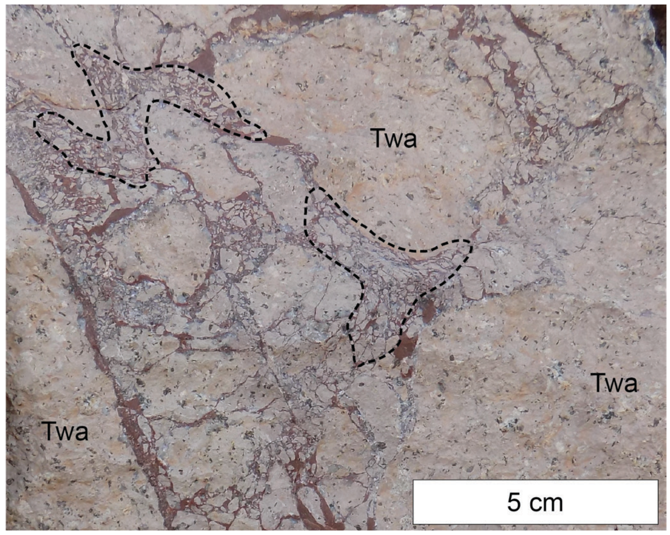

FIGURE 6. Clast alignment in breccias in the fault zone hanging wall. Areas within dotted lines display strongest clast alignment. Red material in interstitial areas is cataclasite interpreted to be reworked sands of the Spears Group. Twa = Andesite of Willow Springs.

fractures also contains fractures in orientations perpendicular to the fault and in random orientation; these fractures have little to no offset and contain no observed cataclasite or mineralization.

Fault-related deformation in the hanging wall is dominated by randomly oriented finer-grained cataclasite- and breccia-filled fractures. Fracture apertures decrease and fracture spacings (i.e., average distance between two fractures) increase away from the fault zone. Centimeter-scale fracture apertures are common in the hanging wall within 1 m of the fault core zone; apertures decrease to mostly mm-scale at a distance of 5 m from the fault core. Fractures are filled with cataclasite similar to that described above as well as very angular clasts of Twa (Fig. 5). Breccia clast diameters range from mm-scale to roughly the aperture of the fracture containing the breccia. Foliation is observed in some but not all breccia clasts (Fig. 6). Breccias falling into the chaotic breccia and mosaic breccia categories of Mort and Woodcock (2008) are observed at the outcrop scale.

Microscopy

Sandstones of Tss at the study site are lithic arkoses containing moderately sorted angular to rounded (predominately subangular) medium silt through granules (predominately very fine sand). Sandstones have an average composition of 50±10% quartz, 30±5% feldspar, and 20±10% lithic fragments. Opaque oxide grains make up 1–3% of Tss. Oxide grains in Tss have an average diameter of 50 µm (n=39), which is less than the average diameter of Tss clasts (96 µm; n=419). Summary clast size data are presented in Table 1.

TABLE 1. Summary of clast size data from cataclasites and Spears Group sandstones.

	Cataclasite	Spears Group Sandstone
Average grain size	65 µm	96 µm
Median grain size	63 µm	80 µm
Standard deviation	24.08	82.43
n	383	419

The compositions of cataclasites in faults and fractures at the study site classify as lithic arkoses and feldspathic litharenites containing moderately to well-sorted angular to rounded (predominately subangular) medium silt through fine sand (predominately very fine sand). Cataclasites have an average composition of 55±10% quartz, 10±4% feldspar, and 35±8% lithic fragments. Cataclasites display internal sorting based on clast size and composition (Fig. 7). Weak layering is present in some cataclasites, but random clast orientations predominate. Cataclasites fill fractures in Twa with apertures as small as 50 µm. Shear zones and the boundaries of competent clasts of Twa are sometimes but not always marked with 10–30 µm-thick zones of very fine silt- to clay-sized particles interpreted here as ultracataclasite *sensu* Davis et al. (2014) after Sibson (1977).

Some zones of cataclasites at the study site exhibit concentration of oxide mineral clasts far beyond that observed in Tss (Figs. 7, 8). Zones of oxide concentration are 0.1–1.1 mm thick and are elongated to at least 26 mm; their total length is currently unknown due to observation limitations on a standard

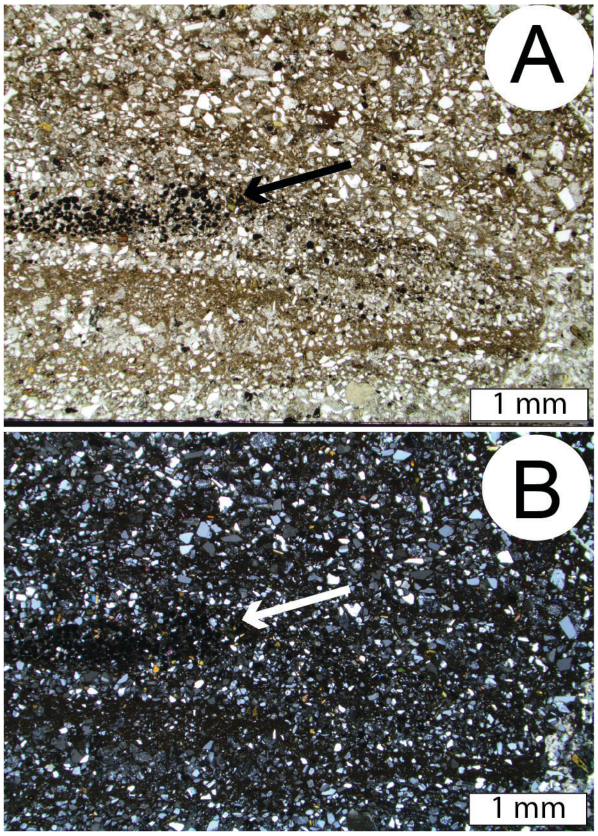

FIGURE 7. Plane light (A) and cross-polarized light (B) photomicrographs of a zone of oxide concentration (denoted by arrow) within cataclasite in the fault zone. In (A), bands of size-segregated materials are also visible roughly parallel to the zone of oxide concentrations. Note range of grain rounding from angular to subrounded.

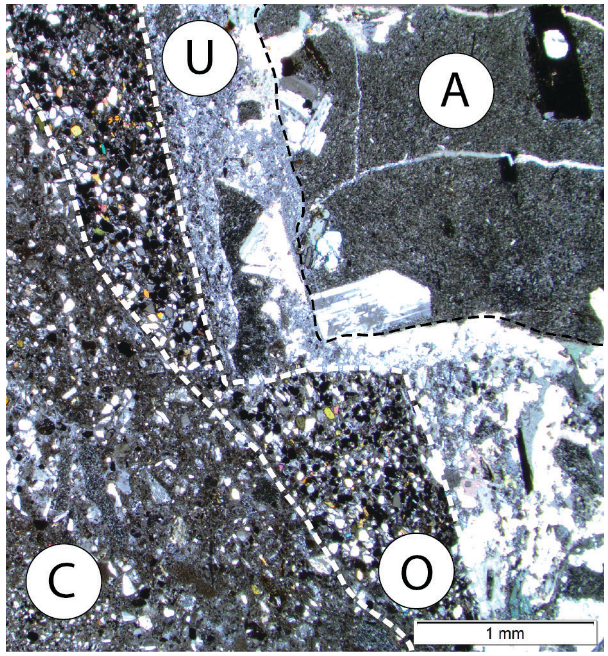

FIGURE 8. Cross-polarized light photomicrograph of complex fracture boundary from the fault zone hanging wall. A = microfractured andesite with plagioclase phenocrysts. U = ultracataclasite with some larger fractured clasts. O = zone of oxide clast concentration. C = 'typical' fine-grained cataclasite of similar mineral composition to Spears Group sandstones.

26 x 46 mm petrographic thin section. Zones of oxide concentration occur both in contact with andesite as well as within cataclasite not in contact with andesite. Individual oxide grains in cataclasites have the same average size and rounding as those in Tss. Besides the high concentration of oxide clasts, there are no obvious other chemical, textural, or compositional differences between the zones of oxide concentration and other cataclasites at the study site. Cataclasites contain 0.5–3% oxide grains outside of the zones of oxide concentration.

X-ray Diffraction

Diffractograms and graphic representations of diffractogram relative peak strength for four analyzed samples are presented in Figure 9. In both analyzed Tss samples, the predominant identified minerals are quartz, albite, augite, and a zeolite mineral (likely stellerite). The same mineral assemblages were identified via XRD in both cataclasite samples.

DISCUSSION

The composition, grain size, mineralogy, and orientation of cataclasites at the study site suggest that they were created from incorporation of Tss into the fault zone during faulting, at least partly through particulate flow processes. Andesites in the fault walls contributed granules and coarser material as breccia clasts into the fault zone, but fault zone materials that are finer than medium sand appear to have been sourced solely from Tss. This might indicate that faulting occurred before Tss was well-lithified, and that unlithified sediments were able to enter incipient fractures as they opened during faulting. Cataclasis in unlithified or poorly lithified sediments is reported in various geologic settings (Lucas and Moore, 1986; Cashman and Cashman, 2000; Rawling and Goodwin, 2003). Rawling and Goodwin (2006) report poorly lithified sand being incorporated into Santa Fe Group fault zones of roughly the same dimensions as the one reported here; these fault zone sands sometimes retain primary sedimentary structures despite moderate structural deformation related to faulting. Unlike Rawling and Goodwin (2006), where sands incorporated into the fault zone can be linked to a bed in the footwall or hanging wall over vertical distances of meters or less, it is unclear in this study precisely how far Tss sands might have been transported into the fault zone during deformation.

Cataclasites at the study quarry show a lower average clast size and higher degree of sorting than does Tss (Table 1). Grain size reduction in shear and dilation zones in sandstones and poorly lithified sands are reported at multiple scales (e.g., Wu and Groshong, 1991; Fisher et al., 2003; O'Kane et al., 2007). There are several potential explanations for the observed grain-size reductions at the study site. First, perhaps the cataclastic material was sourced from a portion of Tss that was anomalously finer grained and better sorted than those portions sampled for this study. Given the limited exposures at the study site, this hypothesis cannot be tested with currently available surface exposures. Second, cataclasites might have originated

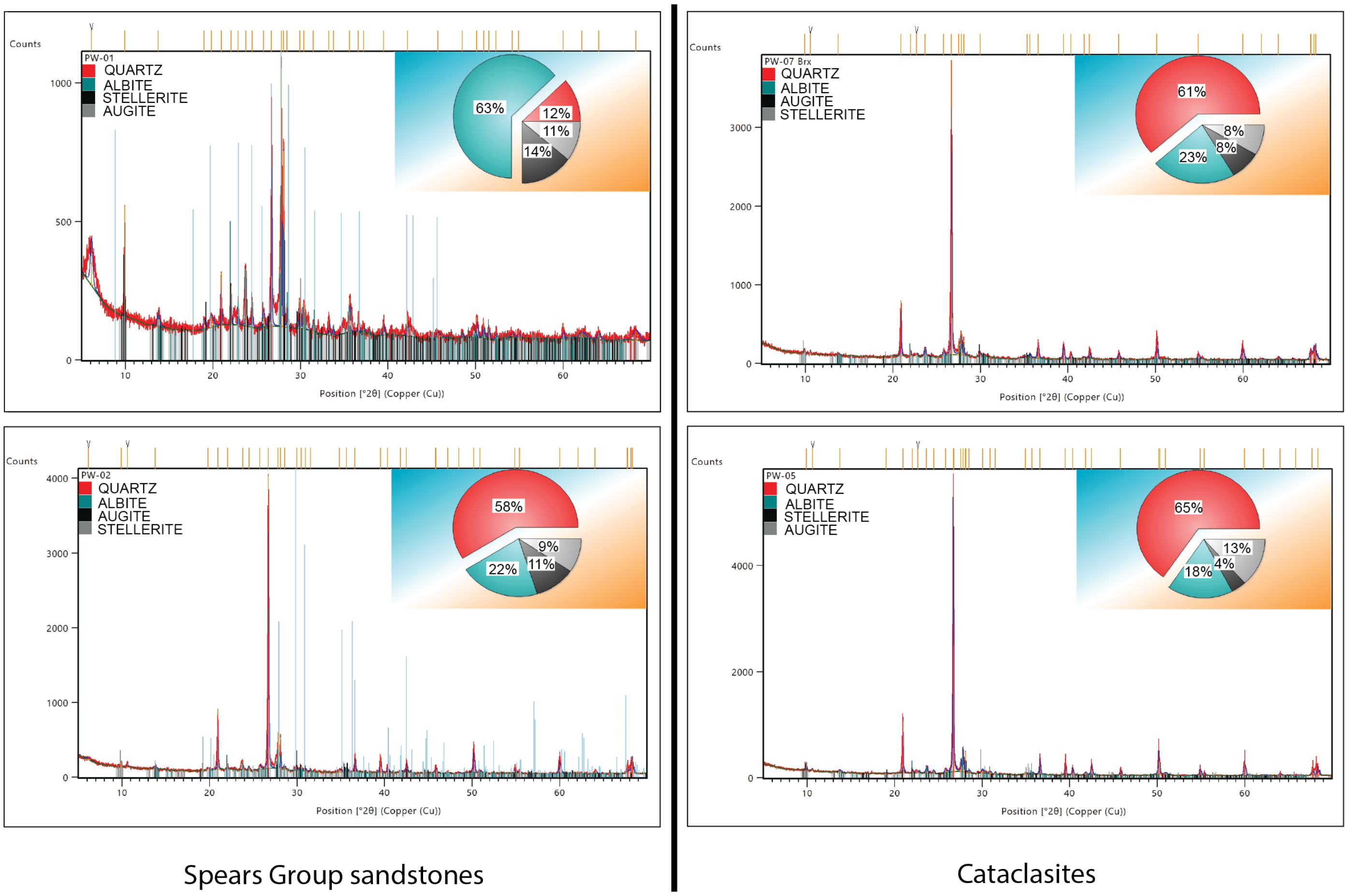

FIGURE 9. Interpreted diffractograms of whole-rock samples. Sample ID PW-01 and PW-02 are Spears Group sandstones. Sample ID PW-07 Brx and PW-05 are cataclasites collected from within fractures in the fault zone hanging wall.

in a Tss source of the same clast size and sorting as was sampled for this study, but smaller clasts were preferentially incorporated into the fault zone. Clast segregation is observed within cataclasites at the study site (e.g., Figs. 7, 8), but whether segregation occurred during the cataclasites' sourcing from Tss or after incorporation into the fault zone is unknown. Third, the cataclasites' average clast diameter was reduced via brittle failure of individual grains during strain accumulation. Biegel et al. (1989) and Hooke and Iverson (1995) show that in unlithified clastic sediment in heterogenous stress fields, individual clasts may accommodate strain via spalling (fracturing of rock caused by interaction of compression at a free surface, accompanied by the outward heaving of the fractured particle, similar to exfoliation), transgranular fracture, or intragranular microcracking. Rawling and Goodwin (2003) point to these strain accommodation models, particularly spalling of quartz grains, as a likely cause for the reduction in particle size distribution values observed in Santa Fe Group sands in fault zones in the Albuquerque Basin. Transgranular fracture in fault rock material is relatively uncommon and mineralogy dependent in some Santa Fe Group faults (Rawling and Goodwin, 2003), and the apparent lack of transgranular fracture in feldspars observed in this study also suggests quartz spalling plays a major role in reduction of grain size in cataclasites. Further analysis and larger sample sizes are necessary in order to conclude that these processes are responsible for the grain size and sorting observations reported here. Further work also is needed to determine whether comminution observed here is best explained by unconstrained or constrained models *sensu* Sammis et al. (1987). In faults cutting uniform rock types, the presence of fault breccias alongside finer-grained cataclasites are a non-unique criteria to evaluate the state of cohesion during fault motion but suggest burial at relatively shallow depths (Sibson, 1977). Given the interlayered relationship between Twa and Tss at the study site and the different mechanical properties of these two units, multiple stages of motion likely are not necessary for creation of the observed features, though they cannot be ruled out. The relatively large fracture apertures, boulders, cobbles, and rounding observed in this fault seem to indicate near-surface conditions.

The concentration of oxides in some zones of cataclasites at the study site is peculiar. The simplest explanation is that these zones of oxide concentration represent original bedding from Tss that was enriched in oxides and transported into cataclasite via particulate flow of disaggregated sediment. Spears Group sandstones contain Fe-Ti oxide detrital grains (Chamberlin et al., 1994), but the presence of placer concentration of oxides in the Spears Group is unknown. Heynekamp et al. (1999) and Rawling and Goodwin (2003) report bedding from poorly lithified faulted sediments being transported into fault zones as cataclasite in Rio Grande rift–related normal faults. However, no beds of higher-than-average oxide (or denser-than-average) clast concentration are observed in Tss at the study site. This does not rule out their existence elsewhere in the section; the exposed outcrop of Tss is small, and lateral and vertical variations in composition are not unlikely in volcaniclastic sedimentary depositional environments. Another potential explanatory process for oxide concentration is pressure solution creep, by which soluble minerals such as quartz or feldspars are progressively dissolved in high-pressure fluids and removed from the fault zone by fluid flow. This leads to a passive concentration of insoluble minerals such as phyllosilicates or oxides (Weyl, 1959; Paterson, 1973). This process is reported in some faults in the upper crust (Gratier et al., 2013, and references therein; Pei et al., 2015). This process is not suspected at the study site, since the zones of oxide concentration also contain undeformed quartz and feldspar grains that show no evidence of having undergone pressure solutions. The presence of zones of oxide concentration in cataclasites at the study site remains unexplained and warrants further explanation.

Syntectonic calcite mineralization in Rio Grande rift–related fault zones is reported by Williams et al. (2015), but further work is needed at this study site to determine more precisely the timing of calcite mineralization relative to fault motion. Fluid inclusions in calcite at the study site (Fig. 3) are a potential target for future fault-related fluid investigations via LA-ICP-MS (A. Gysi, pers. commun., 2022).

CONCLUSIONS

Textural and mineralogical data presented here indicate that faulting of Eocene andesites in the southernmost Chupadera Mountains caused mobilization of interlayered and similarly aged sands and silts of the Spears Group into the fault zone. Pressure conditions during faulting are interpreted to have caused these sediments to flow into and fill fractures with apertures at least as small as the diameter of the average grain size of the sediment. Andesites in the fault walls are fractured and, to a lesser extent, brecciated; however, andesite was not mobilized into fractures in the form of fine-grained cataclasite as was Tss. Sediments of the Spears Group interpreted to have been transported into the fault zone are of smaller average diameter than nearby in situ Spears Group sandstones; cataclasis during mobilization into the fault zone is a potential cause for observed grain-size reduction. As is reported in other Rio Grande rift–related faults in poorly consolidated siliciclastic sediments, reduction in clast diameters likely occurred primarily through quartz spalling during grain-to-grain comminution. Further analysis at the site is needed to determine potential timing of faulting and of post-faulting calcite mineralization. Future studies at this site, which is one of the only outcrops of faulted bedrock in the San Marcial Basin, can increase understanding not only of the basin's tectonic development, but also of fault behavior in interbedded volcanic/sedimentary sequences that are common in active tectonic settings.

ACKNOWLEDGMENTS

Dan Koning observed these outcrops and exposures during geologic mapping on the Fort Craig 7.5-minute quadrangle and suggested further study. This manuscript stems from that suggestion. Alex Gysi and Matt Zimmerer provided guidance with photomicroscopy. Conversations with Snir Attia and Jacob Thacker led to insights into fault mechanics, processes, and products. Jonathan Saul Caine and Geoff Rawling provided helpful reviews that improved an earlier draft of this manuscript.

REFERENCES

Abbey, A.L., and Niemi, N.A., 2020, Perspectives on continental rifting processes from spatiotemporal patterns of faulting and magmatism in the Rio Grande rift, USA: Tectonics, v. 39, no. 1, p. e2019TC005635.

Biegel, R.L., Sammis, C.G., and Dieterich, J.H., 1989, The frictional properties of a simulated gouge having a fractal particle distribution: Journal of Structural Geology, v. 11, no. 7, p. 827–846.

Blenkinsop, T.G., 1991, Cataclasis and processes of particle size reduction: Pure and Applied Geophysics, v. 136, no. 1, p. 59–86.

Bolognesi, F., and Bistacchi, A., 2016, Weakness and mechanical anisotropy of phyllosilicate-rich cataclasites developed after mylonites of a low-angle normal fault (Simplon Line, Western Alps): Journal of Structural Geology, v. 83, p. 1–12.

Cashman, S., and Cashman, K., 2000, Cataclasis and deformation-band formation in unconsolidated marine terrace sand, Humboldt County, California: Geology, v. 28, no. 2, p. 111–114.

Chamberlin, R.M., Cather, S.M., Anderson, O.J., and Jones, G.E., 1994, Reconnaissance geologic map of the Quemado 30 x 60 minute quadrangle, Catron County, New Mexico: New Mexico Bureau of Mines and Mineral Resources, Open-file Report 406, 30 p., 2 plates.

Chapin, C.E., and Cather, S.M., 1994, Tectonic setting of the axial basins of the northern and central Rio Grande rift, *in* Keller, C.G., and Cather, S.M., eds., Basins of the Rio Grande Rift: Structure, Stratigraphy, and Tectonic Setting: Boulder, Colorado, Geological Society of America, Special Paper 291, p. 5–25.

Cikoski, C.T., Roth, S.J., and Osburn, G.R., 2013, Geologic Map of the Cienega Ranch Quadrangle, Socorro County, New Mexico: New Mexico Bureau of Geology and Mineral Resources, Open-file Geologic Map 239, scale 1:24,000.

Davis, G.H., Constenius, K.N., Dickinson, W.R., Rodríguez, E.P., and Cox, L J., 2004, Fault and fault-rock characteristics associated with Cenozoic extension and core-complex evolution in the Catalina-Rincon region, southeastern Arizona: Geological Society of America Bulletin, v. 116, no. 1-2, p. 128–141.

Davis, G.H., Rodriguez, E.P., Cox, L.J., Ornelas, R., Constenius, K.N., Johnson, J.A., Kong, F., Bedford, J.M., and Pecha, M., 2014, 6. Cohesive Crush Breccias, Microbreccias, and Cataclasites in Granitic Foota/Vall of a Normal Fault, *in* Arthur, W.S., Jan, T., and Victoria, R.T., eds., Fault-related Rocks: A Photographic Atlas: Princeton University Press, p. 36–37.

Dickinson, W.R., 1970, Interpreting detrital modes of graywacke and arkose: Journal of Sedimentary Research, v. 40, no. 2, p. 695–707.

Engelder, J.T., 1974, Cataclasis and the generation of fault gouge: Geological Society of America Bulletin, v. 85, no. 10, p. 1515–1522.

Fisher, Q.J., Casey, M., Harris, S.D., and Knipe, R.J., 2003, Fluid-flow properties in sandstone: The importance of temperature history: Geology, v. 31, p. 965–968.

Gallant, K.R., Rinehart, A., Koning, D.J., 2022, Inferences on the structure and geometry of the San Marcial Basin using gravity data: New Mexico Geological Society, this volume.

Gratier, JP., Dysthe, D.K., and Renard, F., 2013, The role of pressure solution creep in the ductility of the Earth's upper crust: Advances in Geophysics, v. 54, p. 47–179.

Hadizadeh, J., Babaie, H.A., and Babaei, A., 1991, Development of interlaced mylonites, cataclasites and breccias: example from the Towaliga fault, south central Appalachians: Journal of Structural Geology, v. 13, no. 1, p. 63–70.

Heynekamp, M.R., Goodwin, L.B., Mozley, P.S., and Haneberg, W.C., 1999, Controls on fault-zone architecture in poorly lithified sediments, Rio Grande Rift, New Mexico: Implications for fault-zone permeability and fluid flow, *in* Haneberg, W.C., et al., eds., Faults and Subsurface Fluid Flow in the Shallow Crust: Geophysical Monograph Series, v. 113, p. 27–49.

Hooke, R.L., and Iverson, N.R., 1995, Grain-size distribution in deforming subglacial tills: role of grain fracture: Geology, v. 23, no. 1, p. 57–60.

Jébrak, M., 1997, Hydrothermal breccias in vein-type ore deposits: a review of mechanisms, morphology and size distribution: Ore Geology Reviews, v. 12, no. 3, p. 111–134.

Koning, D.J., Pearthree, K.S., Jochems, A.P., and Love, D.W., 2020, Geologic map of the San Marcial 7.5-minute Quadrangle, Socorro County, New Mexico: New Mexico Bureau of Geology and Mineral Resources, Open-file Geologic Map 287, scale 1:24,000.

Koning, D.J., Hobbs, K.M., Pearthree, K.S., and Love, D.W., 2021, Geologic map of the Fort Craig 7.5-minute quadrangle, Socorro County, New Mexico: New Mexico Bureau of Geology and Mineral Resources, Open-file Geologic Map 288, scale 1:24,000.

Laznicka, P., 1988, Breccias and coarse fragmentites: petrology, environments, associations, ores: New York, Elsevier.

Lucas, S.E., and Moore, J.C., 1986, Cataclastic deformation in accretionary wedges: Deep Sea Drilling Project Leg 66, southern Mexico, and on-land examples from Barbados and Kodiak Islands: Structural Fabric in Deep Sea Drilling Project Cores from Forearcs, v. 166, p. 89.

Luther, A., Axen, G., and Selverstone, J., 2013, Particle-size distributions of low-angle normal fault breccias: Implications for slip mechanisms on weak faults: Journal of Structural Geology, v. 55, p. 50–61.

Machette, M.N., Personius, S.F., Kelson, K.I., Haller, K., and Dart, R., 1998, Map and data for Quaternary faults and folds in New Mexico: U.S. Geological Survey Open-File Report, v. 98, no. 521, p. 443.

Mort, K., and Woodcock, N., 2008, Quantifying fault breccia geometry: dent fault, NW England: Journal of Structural Geology, v. 30, no. 6, p. 701–709.

O'Kane, A., Onasch, C.M., and Farver, J., 2007, The role of fluids in low-temperature, fault-related deformation of quartz arenite: Journal of Structural Geology, v. 29, p. 819–836.

Paterson, M., 1973, Nonhydrostatic thermodynamics and its geologic applications: Reviews of Geophysics, v. 11, no. 2, p. 355–389.

Pei, Y., Paton, D.A., Knipe, R.J., and Wu, K., 2015, A review of fault sealing behaviour and its evaluation in siliciclastic rocks: Earth-Science Reviews, v. 150, p. 121–138.

Rawling, G.C., and Goodwin, L.B., 2003, Cataclasis and particulate flow in faulted, poorly lithified sediments: Journal of Structural Geology, v. 25, no. 3, p. 317–331.

Rawling, G.C., and Goodwin, L.B., 2006, Structural record of the mechanical evolution of mixed zones in faulted poorly lithified sediments, Rio Grande rift, New Mexico, USA: Journal of Structural Geology, v. 28, no. 9, p. 1623–1639.

Ricketts, J.W., Kelley, S.A., Karlstrom, K.E., Schmandt, B., Donahue, M.S., and van Wijk, J., 2016, Synchronous opening of the Rio Grande rift along its entire length at 25–10 Ma supported by apatite (U-Th)/He and fission-track thermochronology, and evaluation of possible driving mechanisms: GSA Bulletin, v. 128, no. 3-4, p. 397–424.

Sammis, C., King, G., and Biegel, R., 1987, The kinematics of gouge deformation: Pure and Applied Geophysics, v. 125, no. 5, p. 777–812.

Sibson, R.H., 1977, Fault rocks and fault mechanisms: Journal of the Geological Society, v. 133, no. 3, p. 191–213.

Sibson, R.H., 1986, Brecciation processes in fault zones: inferences from earthquake rupturing: Pure and Applied Geophysics, v. 124, no. 1, p. 159–175.

Sion, B.D., Phillips, F.M., Axen, G.J., Harrison, J.B.J., Love, D.W., and Zimmerer, M.J., 2020, Chronology of terraces in the Rio Grande rift, Socorro basin, New Mexico: Implications for terrace formation: Geosphere, v. 16, no. 6, p. 1457–1478.

Weyl, P.K., 1959, Pressure solution and the force of crystallization: a phenomenological theory: Journal of Geophysical Research, v. 64, no. 11, p. 2001–2025.

Williams, R.T., Goodwin, L.B., Mozley, P.S., Beard, B.L., and Johnson, C.M., 2015, Tectonic controls on fault zone flow pathways in the Rio Grande rift, New Mexico, USA: Geology, v. 43, no. 8, p. 723–726.

Wise, D., Dunn, D., Engelder, J., Geiser, P., Hatcher, R., Kish, S., Odom, A., and Schamel, S., 1984, Fault-related rocks: Suggestions for terminology: Geology, v. 12, no. 7, p. 391–394.

Woodcock, N., Omma, J., and Dickson, J., 2006, Chaotic breccia along the Dent Fault, NW England: implosion or collapse of a fault void?: Journal of the Geological Society, v. 163, no. 3, p. 431–446.

Wu, S., and Groshong, Jr., R.H., 1991, Low-temperature deformation of sandstone, southern Appalachian fold-thrust belt: Geological Society of America Bulletin, v. 103, p. 861–875.